Computer Assisted Mechanics and Engineering Sciences, 15: 305–318, 2008.

Trefftz functions for 3D stress concentration problems

Zuzana Murčinková
Technical University Košice, Faculty of Manufacturing Technologies with seat in Prešov
Department of Technological Devices Design
Bayerova 1, 080 01 Prešov, Slovak Republic

Vladimír Kompiš, Mário Štiavnický
Academy of the Armed Forces of General Milan Rastislav Štefánik,
Department of Mechanical Engineering
Demänovská 393, 031 01 Liptovský Mikuláš, Slovak Republic

(Received in the final form November 18, 2008)

The paper deals with solution of 3D problems with stress concentration using the Trefftz functions. The modelled stress concentrators are holes and cavities of spherical and ellipsoidal shapes. Moreover, the random spherical cavity microstructure is modelled. The Method of External Finite Element Approximation (MEFEA) is applied to simulate detailed stress state of mentioned stress concentrators. This boundary-type method was developed to build special approximation functions that are associated with surface which causes the stress concentration. The method does not need discretization by classical finite elements, however, instead of elements the domain is divided into Trefftz type subdomains. The displacement and force boundary conditions are met only approximately whereas the governing equations are fulfilled exactly in the volume for linear elasticity, making it possible to assess accuracy in terms of error in boundary conditions.

1. Introduction

Holes and different cavities are frequent structural concentrators. Accurate enough computation of stress field is required in order to evaluate static and dynamic (fatigue) behaviour and bearing capacity of the structure. Such computations, especially in 3D and moreover in problems containing the interaction with other types of stress concentrators (cracks, stiff or weak inclusions, inhomogeneities, etc.), require large computational times and are also cumbersome for preparation of models, especially if volume elements (FEM, FVM) are used for the modelling. Meshless methods working with volume approximation are simpler, but need even more equations than FEM and FVM to achieve similar accuracy [5].

Boundary type formulations (BEM) need to discretize only the surface of the structure, however, the numerical algorithms are more complicated and matrices are full or denser populated than by volume methods. Boundary meshless methods (like MFS) possess advantages of efficiency because of simplicity of formulation and small density of resulting matrices. However, problems with numerical stability and accuracy were discovered if the form of the structure is complicated. All boundary methods use Trefftz functions for approximation of internal variables in their formulation [3]. An exception is the BEM, where the fundamental solution satisfies the governing equations in all points except the source point itself.

In this paper, a Method of External Finite Element Approximation (MEFEA) will be presented to model stress concentration problems. MEFEA is an enhanced classic FEM with idea of external approximations. The method does not need discretization by classical elements, however, instead of elements the domain is divided into Trefftz type subdomains. There are shape functions in the

discrete solution space that do not belong to the infinite dimensional solution space. The domain is split in subdomains (cells) and the approximation is built on each of these subdomains independently of each other. The method is similar to Hybrid Trefftz Finite Element Method, where Trefftz functions are used inside of each element (subdomain). The displacement and force boundary conditions are met only approximately whereas the governing equations are fulfilled exactly in the volume for linear elasticity, making it possible to assess accuracy in terms of error in boundary conditions. The main benefit is that the discretization can be done directly on a 3D CAD geometry with all details (features) for the analysis.

2. The method of weighted residuals (Galerkin's method)

The base of MEFEA is the Method of Weighted Residuals (Galerkin's method) [1]. It is one of the mathematical approaches for obtaining approximate solutions to differential equations. Problems of theory of elasticity, fluids mechanics and mathematical physics are formulated as boundary value problems. The aim is to find an approximate functional representation for field variable $\mathbf{u}$ which fulfils governing equation

$$\mathbf{A}\mathbf{u} = \mathbf{f} \qquad \text{inside domain } \Omega \tag{1}$$

and boundary conditions

$$\mathbf{L}\mathbf{u} = \mathbf{g} \qquad \text{on the boundary } \Gamma \text{ of the domain } \Omega \tag{2}$$

where $\mathbf{A}$ and $\mathbf{L}$ are differential operators.

We approximate field variable $\mathbf{u}$ with $\tilde{\mathbf{u}}$,

$$\mathbf{u} \approx \tilde{\mathbf{u}} = \sum_{i=1}^{m} \mathbf{N}_i \mathbf{c}_i = \mathbf{N}\mathbf{c}, \tag{3}$$

where $\mathbf{N}_i$ are assumed functions, $\mathbf{c}_i$ are unknown coefficients and m is number of unknown coefficients.

Since $\mathbf{u} \neq \tilde{\mathbf{u}}$, then $\mathbf{A}\tilde{\mathbf{u}} - \mathbf{f} \neq 0$. We can write

$$\mathbf{A}\tilde{\mathbf{u}} - \mathbf{f} = \mathbf{R} \tag{4}$$

where $\mathbf{R}$ is the residual (or error). The method of weighted residuals seeks to find the m unknowns $\mathbf{c}_i$ so that $\mathbf{R}$ over all domain is "small".

Unknown coefficients $\mathbf{c}_i$ are calculated from the equation system

$$\int_{\Omega} [\mathbf{A}\tilde{\mathbf{u}} - \mathbf{f}]\mathbf{W}_i \, \mathrm{d}\Omega = \int_{\Omega} \mathbf{R}\mathbf{W}_i \, \mathrm{d}\Omega = 0, \qquad i = 1, 2, \ldots, m, \tag{5}$$

where m is linearly independent weighting function W_i. W_i are chosen to be same as the functions used to approximate $\mathbf{u}$. Thus $W_i = N_i$ for $i = 1, 2, \ldots, m$. If the boundary value problem is linear then Eq. (5) is the system of linear algebraic equations.

The final formulation should be maximal simple using the weak formulation, Green's theorem and suitable weighting functions. In case of Galerkin's method the suitable weighting functions are the same as basis functions.

3. T-polynomials for linear elasticity

The governing differential equilibrium equations in displacements for linear isotropic elastic solid under static load condition (known as Lamé–Navier equations) have the form [2]

$$(\lambda + \mu)u_{k,kj} + \mu u_{j,ii} + \bar{b}_j = 0 \tag{6}$$

where

$$\mu = \frac{E}{2(1+\nu)} \quad \text{and} \quad \lambda = \frac{E\nu}{(1+\nu)(1-2\nu)}, \tag{7}$$

E is modulus of elasticity and ν is Poisson's ratio of material.

The components of the displacement field are expressed as

$$\begin{Bmatrix} u_1 \\ u_2 \\ u_3 \end{Bmatrix} = \begin{bmatrix} \mathbf{P}(\mathbf{x}) & 0 & 0 \\ 0 & \mathbf{P}(\mathbf{x}) & 0 \\ 0 & 0 & \mathbf{P}(\mathbf{x}) \end{bmatrix} \begin{Bmatrix} \mathbf{C}^{(1)} \\ \mathbf{C}^{(2)} \\ \mathbf{C}^{(3)} \end{Bmatrix} \tag{8}$$

where $\mathbf{P}(\mathbf{x})$ is the full polynomial of the n-th order (the initial set of functions)

$$\mathbf{P}(\mathbf{x}) = \{1, x_1, x_2, x_3, \ldots, x_1^n, x_1^{n-1}x_2, \ldots, x_2x_3^{n-1}, x_3^n\} \tag{9}$$

and $\mathbf{C}^{(j)}$ is the vector of unknown coefficients.

The equilibrium equation (6) contains the second derivatives of the displacement. Thus, the terms of the 0-th and 1-st order satisfy this equation automatically. However, the higher order polynomials cannot be chosen arbitrarily in order to satisfy the equilibrium equation (1).

Equation (8) is split into the form

$$\begin{Bmatrix} u_1 \\ u_2 \\ u_3 \end{Bmatrix} = \begin{bmatrix} \mathbf{A}^{(1)} & 0 & 0 \\ 0 & \mathbf{A}^{(2)} & 0 \\ 0 & 0 & \mathbf{A}^{(3)} \end{bmatrix} \begin{Bmatrix} \mathbf{a}^{(1)} \\ \mathbf{a}^{(2)} \\ \mathbf{a}^{(3)} \end{Bmatrix} + \begin{bmatrix} \mathbf{B}^{(1)} & 0 & 0 \\ 0 & \mathbf{B}^{(2)} & 0 \\ 0 & 0 & \mathbf{B}^{(3)} \end{bmatrix} \begin{Bmatrix} \mathbf{b}^{(1)} \\ \mathbf{b}^{(2)} \\ \mathbf{b}^{(3)} \end{Bmatrix} \tag{10}$$

where the matrix $\mathbf{B}$ contains as many terms as many terms has the two order lower polynomial. The terms of each order of the polynomial are computed separately and they are functions of material properties only. As example the third order polynomial terms can be split so that the upper three terms will be included into $\mathbf{B}^{(1)}$ and the lower part terms into $\mathbf{A}^{(1)}$,

$$\begin{array}{ccccc} & & x_1^3 & & \\ & x_1^2x_2 & & x_1^2x_3 & \\ \hline x_1x_2^2 & & x_1x_2x_3 & & x_1x_3^2 \\ x_2^3 & x_2^2x_3 & & x_2x_3^2 & x_3^3 \end{array} \tag{11}$$

The terms for $\mathbf{B}^{(j)}$ and $\mathbf{A}^{(j)}$ are obtained by changing cyclically the component indices and set into Eq. (6). In this way we can obtain the relation

$$[\mathbf{M}(x_i)]\{\mathbf{b}\} + [\mathbf{N}(x_i)]\{\mathbf{a}\} = \{\mathbf{0}\}. \tag{12}$$

The vector $\mathbf{b}$ contains dependent coefficients which have to be expressed through the independent coefficients $\mathbf{a}$ in order to satisfy the equilibrium equations in each point.

The solution of this problem can be done analytically or numerically. In the last case, we choose so many or more discrete points, as many dependent terms are in the corresponding order of the polynomial (in the given example of the third order polynomial there are at least three points). Note that if more points are chosen than is number of the dependent terms, the system of equations will contain more equations as the number of unknown terms, but it will be not solved in the least square sense, as redundant equations are a combination of the others [2].

We get Eq. (12) in the form

$$[\mathbf{M}({}^{(j)}x_i)]\{\mathbf{b}\} = -[\mathbf{N}({}^{(j)}x_i)]\{\mathbf{a}\} \tag{13}$$

from which we have

$$\{\mathbf{b}\} = -[\mathbf{M}^{-1}][\mathbf{N}]\{\mathbf{a}\}. \tag{14}$$

The upper left index corresponds to the nodal point for determination of coefficients of the T-polynomial displacement. With this, the T-polynomial displacement is

$$\{\mathbf{u}\} = \left([\mathbf{A}(x_i)] - [\mathbf{B}(x_i)]\,[\mathbf{M}^{-1}]\,[\mathbf{N}]\right)\{\mathbf{a}\} = [\mathbf{U}(x_i)]\,\{\mathbf{a}\}. \tag{15}$$

Each column of the matrix $\mathbf{U}$ in Eq. (15) introduces a T-displacement function for each component defined by corresponding row. The T-polynomial contains then one independent term of the polynomial and the dependent terms, too. Note, that in this way, the matrix U contains polynomial terms of both matrices $\mathbf{A}$ and $\mathbf{B}$. The number of T-polynomial functions which can be defined is $(2n+1)$ for 2D and $(n+1)^2$ for 3D problems with n being the polynomial order (containing all orders from 0 to n).

4. Degrees of freedom in MEFEA

In MEFEA the degrees of freedom have no physical meaning comparing with traditional FEM where degrees of freedom are displacement of nodes, temperature, etc. There are three types of degrees of freedom: Boundary DOF, Internal DOF and Concentrator DOF. Concentrator DOFs are functions associated with the surfaces which cause stress concentration. They correspond to the special basic functions intended to accurately simulate the stress state near stress concentration regions.

The special basic functions are $\mathbf{f}_i = \frac{1}{r}$, a concentrator basis function with asymptotic behaviour (radial functions), $i = 1, 2, \ldots, n$ is the number of concentrator degrees of freedom,

$$\mathbf{u} = \sum_{i=1}^{n} \mathbf{N}_i \mathbf{c}_i + \sum_{i=1}^{m} \mathbf{f}_i \mathbf{a}_i\,. \tag{16}$$

Functions $\mathbf{N}_i$ approximate the global behaviour of the structure. Functions $\mathbf{f}_i$ approximate the local behaviour around the holes, different cavities, cracks, stiff or weak inclusions, inhomogeneities and other structural concentrators.

5. Error estimation

Because the basic functions which approximate the displacements of the subdomains exactly fulfill the governing Eq. (1) in the volume, it is then possible to completely characterize the accuracy of the solution through the error in the boundary conditions. The following parameters are controlled during the convergence process: strain energy, error in displacement BC, error in the force BC, error in the continuity conditions for displacement and stresses on the dividers:

- Displacement BC

$$\begin{aligned} \mathbf{U} &= \mathbf{U}^* \\ \mathbf{V} &= \mathbf{V}^* \\ \mathbf{W} &= \mathbf{W}^* \end{aligned} \tag{17}$$

  where $\mathbf{U}^*$, $\mathbf{V}^*$, $\mathbf{W}^*$ are defined components of the displacement on the surface.

- Force BC

$$\begin{aligned} \mathbf{T}_x &= \mathbf{T}_x^* \\ \mathbf{T}_y &= \mathbf{T}_y^* \\ \mathbf{T}_z &= \mathbf{T}_z^* \end{aligned} \tag{18}$$

  where $\mathbf{T}_x^*$, $\mathbf{T}_y^*$, $\mathbf{T}_z^*$ are the defined components of traction on the surface.

On the divider surfaces of the subdomains, there are continuity conditions:

- Continuity of displacement

$$\begin{aligned} \mathbf{U}^+ &= \mathbf{U}^- \\ \mathbf{V}^+ &= \mathbf{V}^- \\ \mathbf{W}^+ &= \mathbf{W}^- \end{aligned} \tag{19}$$

- Force BC

$$\begin{aligned} \mathbf{T}_x^+ &= \mathbf{T}_x^- \\ \mathbf{T}_y^+ &= \mathbf{T}_y^- \\ \mathbf{T}_z^+ &= \mathbf{T}_z^- \end{aligned} \tag{20}$$

where symbols "+" and "-" identify quantities witch correspond to adjacent subdomain.

All conditions can be rewritten as follows,

$$\mathbf{U} - \mathbf{U}^* = \mathbf{0} \qquad \text{on surfaces with defined displacement,} \tag{21}$$

$$\mathbf{T} - \mathbf{T}^* = \mathbf{0} \qquad \text{on surfaces with defined force,} \tag{22}$$

$$\mathbf{U}^+ - \mathbf{U}^- = \mathbf{0} \qquad \text{on divider surfaces,} \tag{23}$$

$$\mathbf{T}^+ - \mathbf{T}^- = \mathbf{0} \qquad \text{on divider surfaces,} \tag{24}$$

where $\mathbf{U} = \begin{Bmatrix} \mathbf{U} \\ \mathbf{V} \\ \mathbf{W} \end{Bmatrix}$ is the displacement vector and $\mathbf{T} = \begin{Bmatrix} \mathbf{T}_x \\ \mathbf{T}_y \\ \mathbf{T}_z \end{Bmatrix}$ is the vector of tractions.

As we have an approximate solution, i.e. there are approximate values U_a and tractions T_a on the boundaries and divider surfaces, so

$$\begin{aligned} \mathbf{U}_a - \mathbf{U}^* &= \mathbf{U}_e \neq \mathbf{0} \\ \mathbf{T}_a - \mathbf{T}^* &= \mathbf{T}_e \neq \mathbf{0} \\ \mathbf{U}_a^+ - \mathbf{U}_a^- &= \mathbf{U}_e^i \neq \mathbf{0} \\ \mathbf{T}_a^+ - \mathbf{T}_a^- &= \mathbf{T}_e^i \neq \mathbf{0} \end{aligned} \tag{25}$$

where $|\mathbf{U}_e|$, $|\mathbf{T}_e|$, $|\mathbf{U}_e^i|$, $|\mathbf{T}_e^i|$ are modules of the vectors and characterize the error in the BC and subdomain continuity conditions.

The modules are calculated at many points on each surface of the structure. This gives the error functions

$$\frac{|\mathbf{U}_e|}{\max \textit{displacement}} 100\%, \qquad \frac{|\mathbf{T}_e|}{\max \textit{stress}} 100\%. \tag{26}$$

Errors in displacement BCs decrease by the increase in boundary DOFs, errors in force BCs decrease by the increase in internal DOFs and by addition of stress concentrator DOFs.

6. Integration over the domain

To build the matrix of dependence the coefficients of initial set of functions and subdomain boundary degrees of freedom of each subdomain, the integration is necessary to do. The Green's theorem is used to calculate the integrals of following type: $\int_\Gamma x_1^m x_2^n \, \mathrm{d}x$.

MEFEA enables to make 3D subdomains of complex form. In this case the subdomains geometry is possible to define through the composition of enough simple surfaces (parts of subdomains boundary). The examples of smooth parts of either the boundary of the part or a divider surface are

plain triangle, quadrangle, planar quadratic triangle, quadrangle and boundaries of higher orders. The different types of smooth parts of either the boundary of the part or a divider surface are defined using parametric equations

$$x_i = \sum_{j=1}^{n} f_j(t)\, x_i^{(j)}, \qquad i = 1, 2, 3, \tag{27}$$

where $t = (t_1, t_2)$, $f_j(t)$ are polynomials and $x_i^{(j)}$ are coordinates of nodes situated on the smooth parts of subdomains boundaries.

For example planar non-linear (quadratic) triangle $n = 6$, $p = 2$:

$$\begin{aligned} &f_1 = t_1(2t_1 - 1); \qquad f_2 = t_2(2t_2 - 1); \qquad f_3 = (1 - t_1 - t_2)(1 - 2t_1 - 2t_2); \\ &f_4 = 4t_1t_2\,; \qquad f_5 = 4t_2(1 - t_1 - t_2); \qquad f_6 = 4t_1(1 - t_1 - t_2). \end{aligned} \tag{28}$$

Boundary DOFs are described by the functional [1]

$$\int_{\partial\Gamma} \mathbf{g}_i \mathbf{N}_i \, \mathrm{d}\gamma \tag{29}$$

where $\partial\Gamma$ is the subdomain boundary, $\mathbf{g}_i$ are functions defined on the subdomain's boundary and $\mathbf{N}_i$ are functions to be approximated.

In the functional (29), $\mathrm{d}\gamma$ is equal to

$$\mathrm{d}\gamma = \sqrt{g_1^2 + g_2^2 + g_3^2}\, \mathrm{d}t \tag{30}$$

where $dt = \mathrm{d}t_1 \mathrm{d}t_2$,

$$g_1 = \frac{\partial x_2}{\partial t_1}\frac{\partial x_3}{\partial t_2} - \frac{\partial x_3}{\partial t_1}\frac{\partial x_2}{\partial t_2}, \qquad g_2 = \frac{\partial x_3}{\partial t_1}\frac{\partial x_1}{\partial t_2} - \frac{\partial x_1}{\partial t_1}\frac{\partial x_3}{\partial t_2}, \qquad g_3 = \frac{\partial x_1}{\partial t_1}\frac{\partial x_2}{\partial t_2} - \frac{\partial x_2}{\partial t_1}\frac{\partial x_1}{\partial t_2},$$

and x_i, $i = 1, 2, 3$ are parametric polynomials (27).

To calculate the integrals $\int_\Gamma x_1^m x_2^n \, \mathrm{d}x$, the Green's theorem is used,

$$\int_\Gamma \left(\frac{\partial v}{\partial x_1} + \frac{\partial u}{\partial x_2} \right) \mathrm{d}x = \int_{\partial\Gamma} (v n_1 + u n_2) \, \mathrm{d}\gamma, \tag{31}$$

where n_1, n_2 are cosines of normal line the outward to the subdomain boundary, respectively.

For the term $x_1^m x_2^n$

$$x_1^m x_2^n = \frac{1}{2(m+1)} \frac{\partial x_1^{m+1} x_2^n}{\partial x_1} + \frac{1}{2(n+1)} \frac{\partial x_1^m x_2^{n+1}}{\partial x_2}, \tag{32}$$

then

$$\int_\Gamma x_1^m x_2^n \, \mathrm{d}x = \frac{1}{2} \int_{\partial\Gamma} \left(\frac{x_1^{m+1} x_2^n}{m+1} n_1 + \frac{x_1^m x_2^{n+1}}{n+1} n_2 \right) \mathrm{d}\gamma. \tag{33}$$

Building of the matrix of products between the initial set of functions (9) and boundary DOFs (29) for each subdomain is required in order to build the final set of T-polynomials and thereafter the stiffness matrix.

7. Numerical results — 3D stress concentration problems

In the following, 3D problems with stress concentration using the Trefftz functions are presented. The modeled stress concentrators are holes and cavities of spherical and ellipsoidal shapes. Moreover, the random spherical cavity microstructure is modelled. The Method of External Finite Element Approximation (MEFEA) is applied to simulate detailed stress state of mentioned stress concentrators. The results are compared with both analytical solution (if it exists) and p-version of classical FEM (pFEM). With p-version of FEM, local areas of stress concentration are simulated by elements with high polynomial order. To refine the approximate solution, the element size is kept constant and element p-order is increased.

7.1. 3D Kirsch problem

The problem shown in Fig. 1 illustrates the state of stress in the vicinity of a cavity by uniaxial stress in infinity. The problem is modelled for $a = 1\,\text{mm}$, $b = 10\,\text{mm}$, $p = 1\,\text{MPa}$ and $\nu = 0.27$. The analytical solution for normal stress σ_{yy} in plane $y = 0$ is given as [4]

$$\sigma_{yy} = p\left[1 + \frac{4-5\nu}{2(7-5\nu)}\left(\frac{a}{r}\right)^3 + \frac{9}{2(7-5\nu)}\left(\frac{a}{r}\right)^5\right] \tag{34}$$

where r is the radial distance from centre of the cube to the point of interest.

Figure 2 shows the comparison among the analytical solution and numerical solutions presented by pFEM and MEFEA. The domain is meshed by 1301 p-elements (tetrahedrons) with maximum order 4 and the domain is split by 28 subdomains (Fig. 3) with order 4.

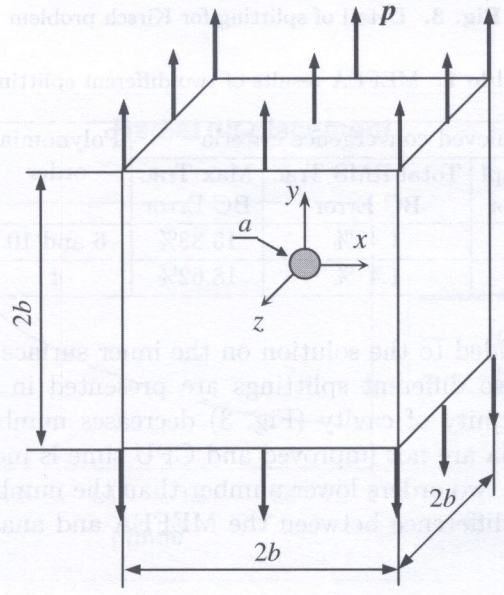

Fig. 1. 3D Kirsch problem

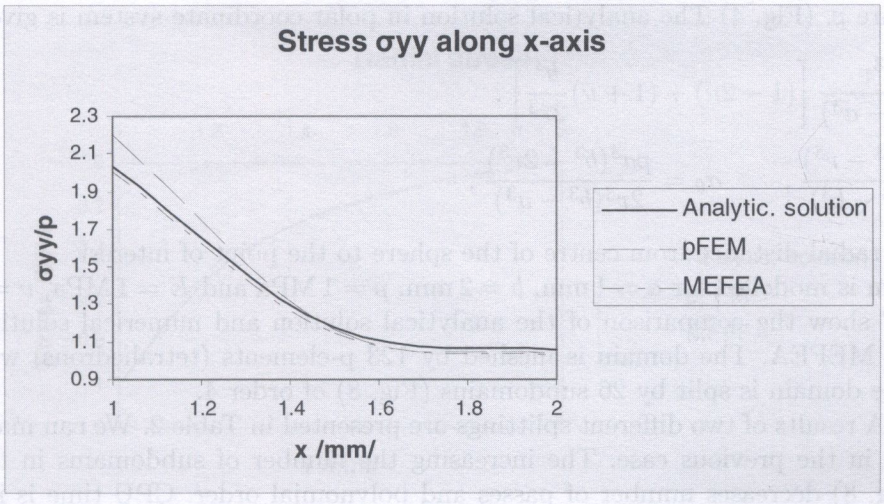

Fig. 2. Comparison of σ_{yy} along the x-axis for Kirsch problem

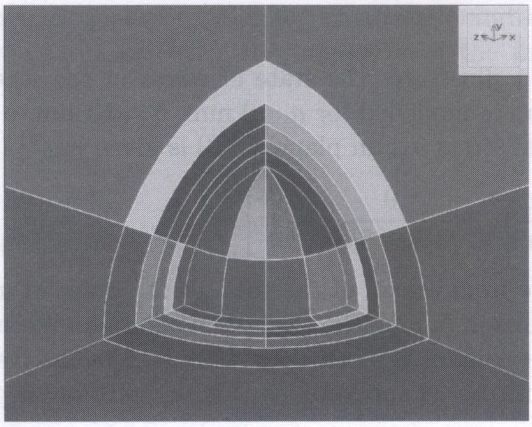

Fig. 3. Detail of splitting for Kirsch problem

Table 1. MEFEA results of two different splittings

Variant	Number of subdomains	Achieved convergence criteria			Polynomial order	Number of passes	Max. stress yy [MPa]	Time
		Max Displ BC Error	Total RMS Trac BC Error	Max Trac BC Error				
A	4	0.94%	1.42%	15.83%	6 and 10	8	1.74	12 s
B	28	0.9 %	1.4 %	18.62%	4	3	2.00	22 s

Stress concentrators are added to the solution on the inner surface of cavity.

The MEFEA results of two different splittings are presented in Table 1. The increasing the number of subdomains in vicinity of cavity (Fig. 3) decreases number of passes and polynomial order. The convergence criteria are not improved and CPU time is increased. However the number of subdomains increased, it is two orders lower number than the number of p-elements in using the same polynomial order. The difference between the MEFEA and analytical maximum stress yy is 1.5%.

7.2. 3D Lame problem

3D Lame problem consists of a hollow sphere with inner radius a and outer radius b loaded by internal pressure p. (Fig. 4) The analytical solution in polar coordinate system is given as [4]

$$u_r = \frac{pa^3 r}{E(b^3 - a^3)} \left[(1 - 2\nu) + (1 + \nu) \frac{b^3}{2r^3} \right], \tag{35}$$

$$\sigma_r = \frac{pa^3(b^3 - r^3)}{r^3(a^3 - b^3)}, \qquad \sigma_\theta = \frac{pa^3(b^3 + 2r^3)}{2r^3(b^3 - a^3)}, \tag{36}$$

where r is the radial distance from centre of the sphere to the point of interest.

The problem is modelled for $a = 1\,\text{mm}$, $b = 2\,\text{mm}$, $p = 1\,\text{MPa}$ and $E = 1\,\text{MPa}$, $\nu = 0.3$.

Figures 5–7 show the comparison of the analytical solution and numerical solutions presented by pFEM and MEFEA. The domain is meshed by 123 p-elements (tetrahedrons) with maximum order 4 and the domain is split by 26 subdomains (Fig. 8) of order 4.

The MEFEA results of two different splittings are presented in Table 2. We can make the similar observation as in the previous case. The increasing the number of subdomains in the vicinity of the cavity (Fig. 8) decreases number of passes and polynomial order. CPU time is increased, but the convergence criteria are improved. However the number of subdomains increased, it is one order lower number than the number of p-elements in using the same polynomial order. The is no difference among MEFEA, pFEM and analytical radial stress results.

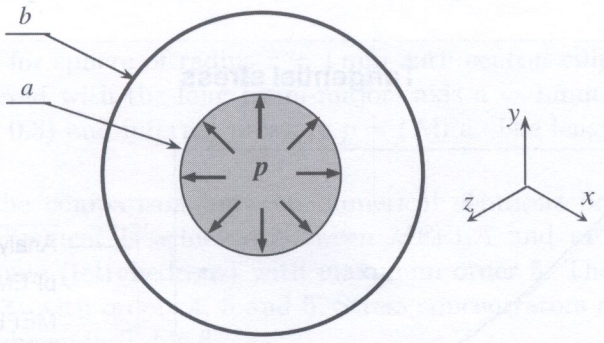

Fig. 4. 3D Lame problem

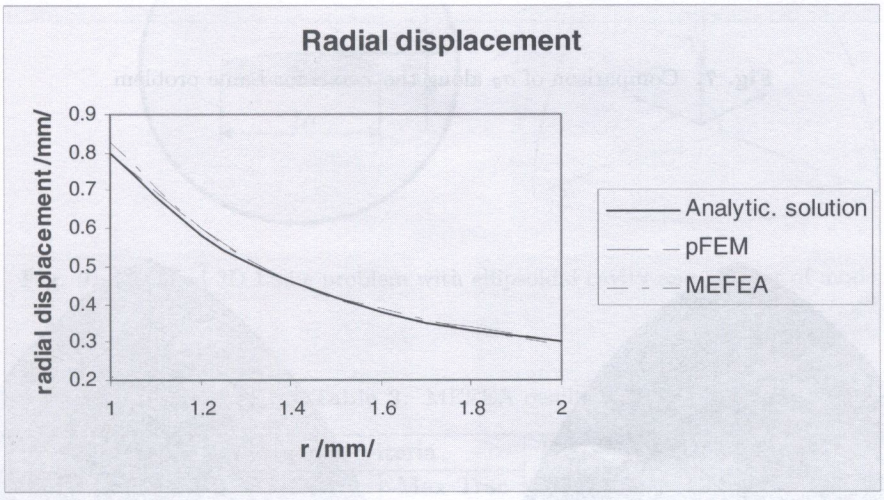

Fig. 5. Comparison of u_r along the x-axis for Lame problem

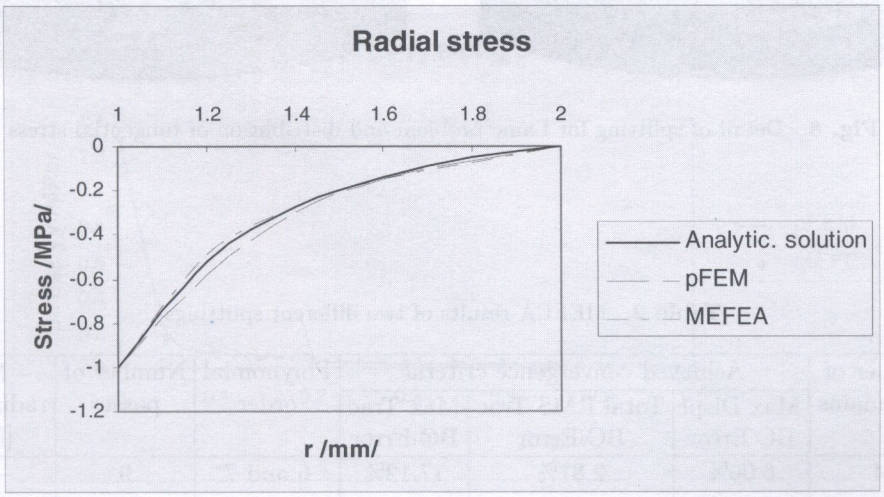

Fig. 6. Comparison of σ_r along the x-axis for Lame problem

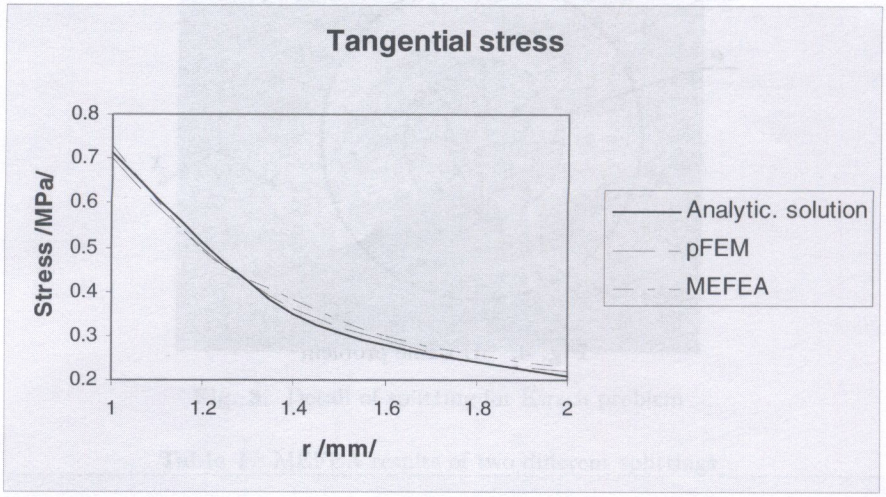

Fig. 7. Comparison of σ_θ along the x-axis for Lame problem

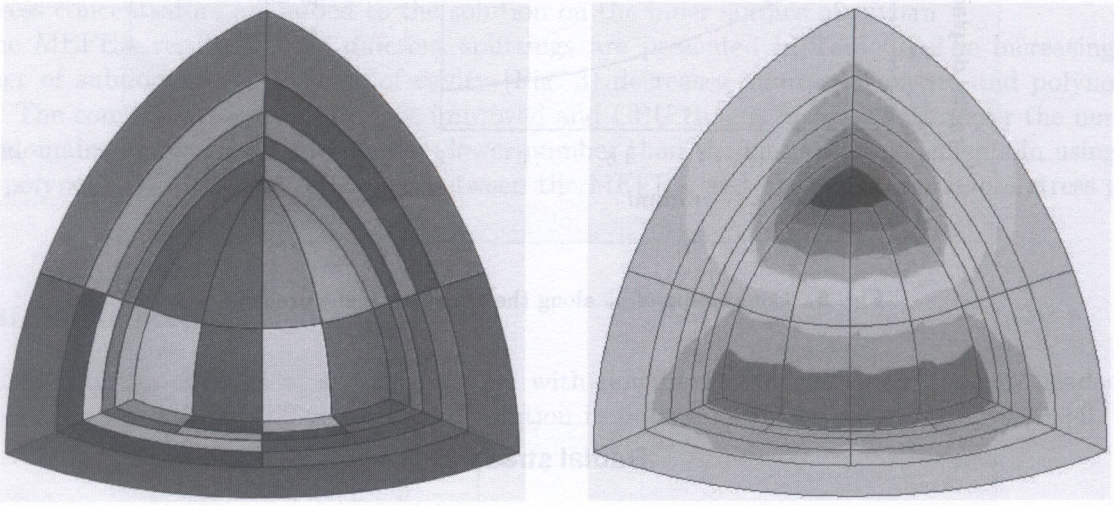

Fig. 8. Detail of splitting for Lame problem and distribution of tangential stress

Table 2. MEFEA results of two different splittings

Variant	Number of subdomains	Achieved convergence criteria			Polynomial order	Number of passes	Max. radial stress [MPa]	Time
		Max Displ BC Error	Total RMS Trac BC Error	Max Trac BC Error				
A	4	6.06%	2.87%	17.12%	6 and 7	9	−0.87	16 s
B	26	3.0 %	2.55%	13.81%	4	8	−1.00	58 s

7.3. Modified 3D Lame problem with ellipsoidal cavity

The problem is modelled for sphere of radius $r = 1\,\text{mm}$ with central ellipsoidal cavity. The cavity is represented as an ellipsoid with the long (semi-major) axis $a = 1\,\text{mm}$ and semi-minor axis $b = 0.2\,\text{mm}$ ($E = 1\,\text{MPa}$, $\nu = 0.3$) and internal pressure $p = 1\,\text{MPa}$. The length of the ellipse is $2a$ and its width is $2b$ (Fig. 9).

Figures 10–12 show the comparison between numerical solutions presented by MEFEA and pFEM. The very fine agreement is achieved between MEFEA and pFEM results. The domain is meshed by 267 p-elements (tetrahedrons) with maximum order 5. The MEFEA model consists of 79 subdomains (Fig. 13) with orders 4, 5 and 6. Stress concentrators are added to the solution. The MEFEA results are shown in Table 3.

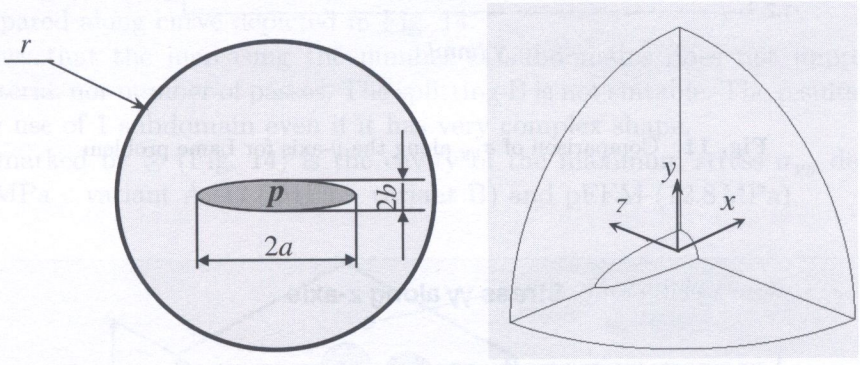

Fig. 9. Modified 3D Lame problem with ellipsoidal cavity and quarter of model

Table 3. MEFEA results

Number of subdomains	Achieved convergence criteria			Polynomial order	Number of passes	Max. stress yy [MPa]	Time
	Max Displ BC Error	Total RMS Trac BC Error	Max Trac BC Error				
79	2.63%	0.63%	30.00%	4, 5, 6	6	1.32	159 s

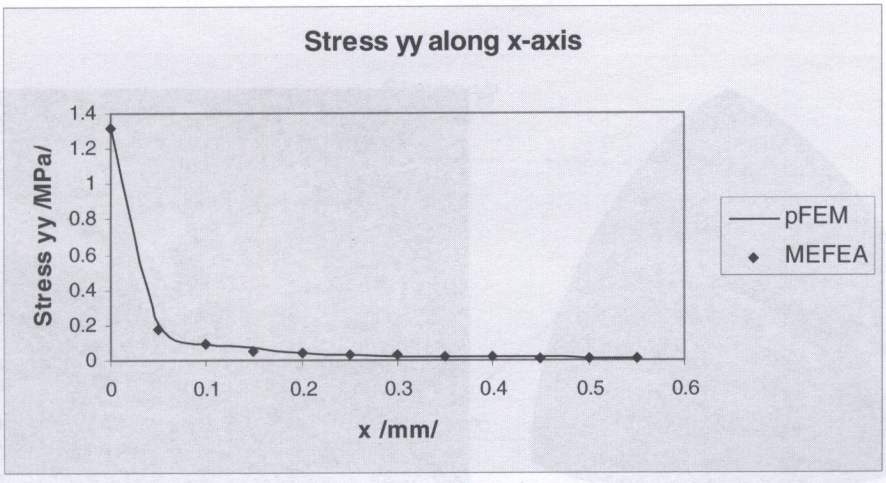

Fig. 10. Comparison of σ_{yy} along the x-axis for Lame problem

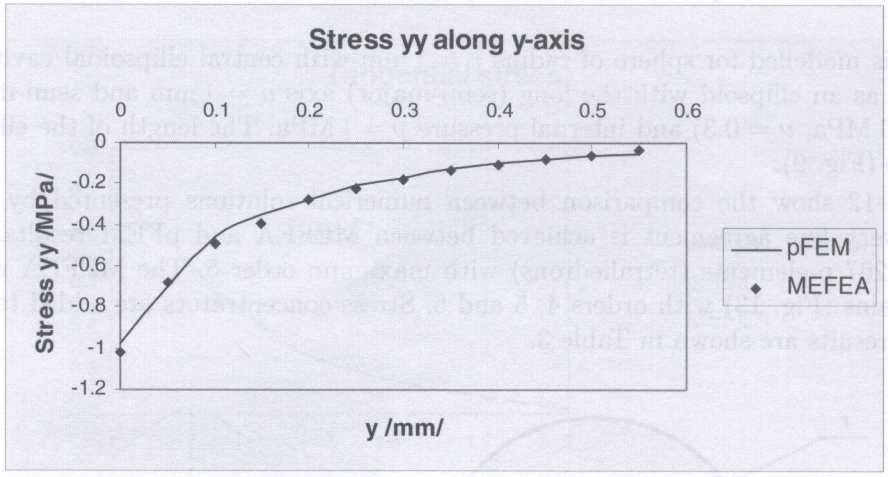

Fig. 11. Comparison of σ_{yy} along the y-axis for Lame problem

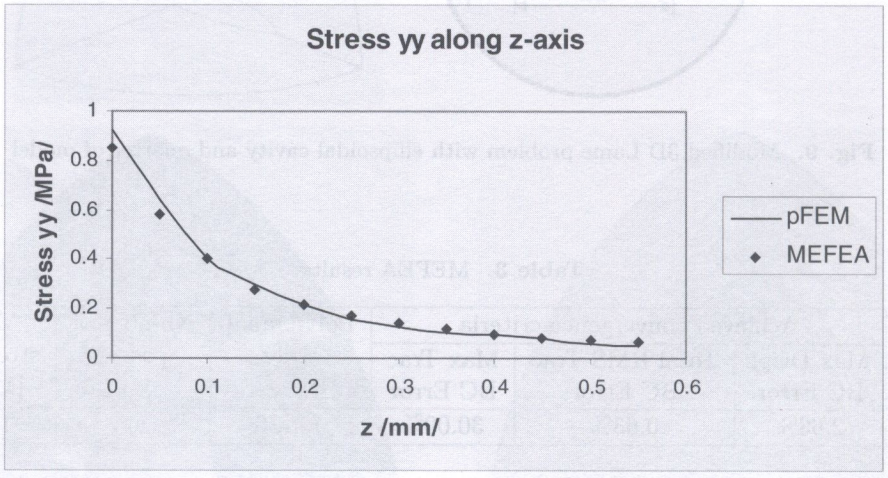

Fig. 12. Comparison of σ_{yy} along the z-axis for Lame problem

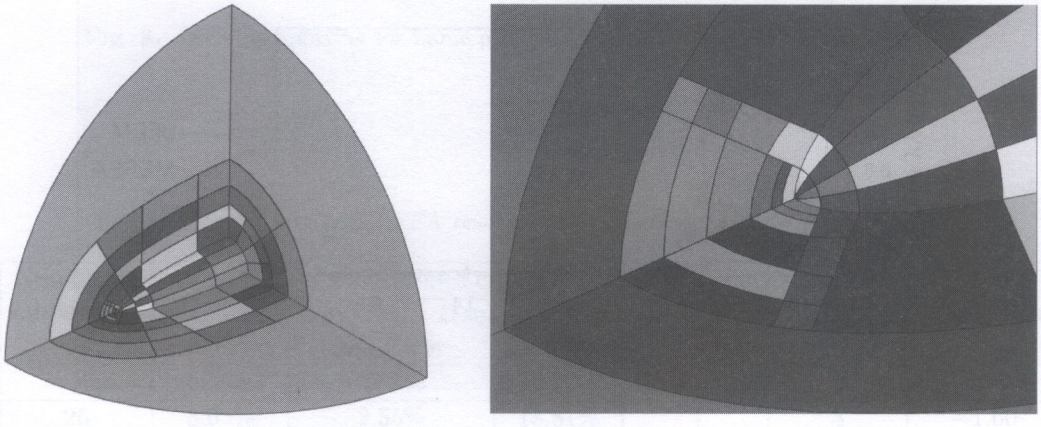

Fig. 13. Splitting and its detail

7.4. 3D random spherical cavity microstructure

3D random spherical cavity micro-structure is representative of more complex structure (Fig. 14). The discontinuities are spherical cavities with diameter $d = 0.4\,\text{mm}$. The control volume of microstructure consists of 16 randomly situated cavities of the same size. The size of control volume is $b = 2\,\text{mm}$. The upper surface has prescribed displacement $u_y = 5 \times 10^5\,\text{mm}$. The symmetry conditions are applied for all other surfaces of control volume. Modulus of elasticity $E = 2 \times 10^5\,\text{MPa}$ and $\upsilon = 0.27$. Whereas the analytical solution does not exist for such problem, the comparison results are results computed by pFEM.

Figure 15 shows the comparison between numerical solutions presented by MEFEA and pFEM. The domain is meshed by 1963 p-elements (tetrahedrons) with maximum order 7. The MEFEA model consists of only 1 subpart with order 4. Stress concentrators are added to the solution. The results are compared along curve depicted in Fig. 14.

Table 4 shows that the increasing the number of subdomains does not improve neither the convergence criteria, nor number of passes. The splitting B is not suitable. The results for comparison are achieved by use of 1 subdomain even if it has very complex shape.

The cavity marked by $\otimes$ (Fig. 14) is the cavity of the maximum stress σ_{yy} detected by both MEFEA (12.0 MPa – variant A, 12.5 MPa – variant B) and pFEM (12.8 MPa).

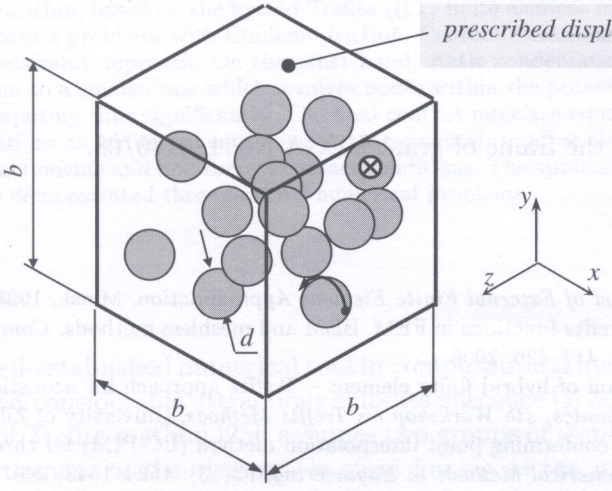

Fig. 14. 3D random spherical cavity microstructure

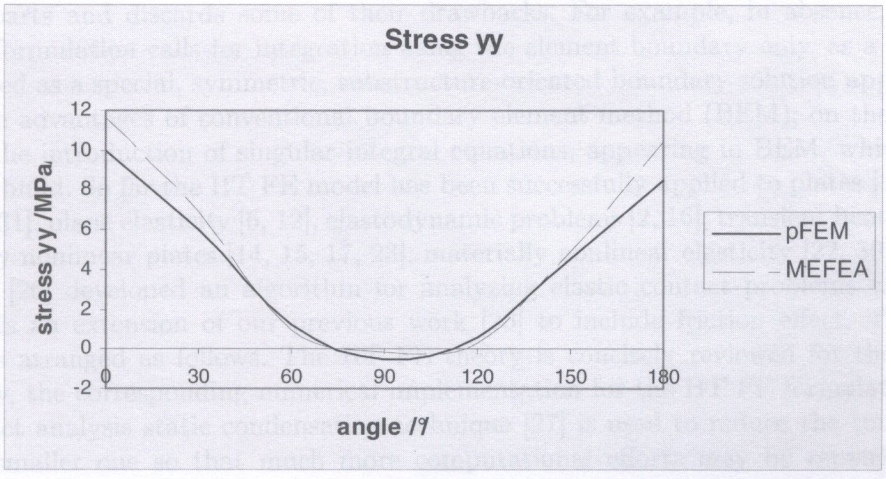

Fig. 15. Comparison of stress σ_{yy}

Table 4. MEFEA results of two different splittings

Variant	Number of subdomains	Achieved convergence criteria			Polynomial order	Number of passes	Max. stress yy [MPa]	Time
		Max Displ BC Error	Total RMS Trac BC Error	Max Trac BC Error				
A	1	2.13%	1.27%	3.84%	4	3	12.0	38 s
B	17	1.06%	3.39%	20.43%	4	10	12.5	501 s

8. Conclusions

In this paper, the computational simulation of holes and different cavities of spherical and ellipsoidal shapes as frequent structural concentrators was performed using classical displacement FEM formulation using p-refinement and a Trefftz-type FEM formulation called the Method of External Finite Element Approximation (MEFEA). The use of large T-elements makes possibility to reduce the problem and also reduce the number of subdomains. However, the special stress concentration functions and mentioned large T-elements are used; the higher density of subdomains is needed to appropriately simulate stress state.

We will continue in this research and the present results will be used for further development of simulation materials with microstructure.

Acknowledgements

The work was carried out in the frame of grant VEGA No. 1/0140/08.

References

[1] V.N. Apanovitch: *The Method of External Finite Element Approximation.* Minsk, 1991.

[2] V. Kompiš, M. Štiavnický. Trefftz functions in FEM, BEM and meshless methods. *Computer Assisted Mechanics and Engineering Science*, **13**: 417–426, 2006.

[3] B. Pluymers *et al.* Application of hybrid finite element – Trefftz approach for acoustic analysis. In: *Numerical Methods in Continuum Mechanics, 4th Workshop on Trefftz Methods*, University of Žilina, Žilina, 2005.

[4] G.Y. Zhang *et al.* A linearly conforming point interpolation method (LC-PIM) for three-dimensional problems. *International Journal for Numerical Methods in Engineering*, **72**(13): 1524–1543, 2007.

[5] M. Žmindák, P. Novák. Meshless methods for analysis of composites reinforced by rigid inclusions. In: *Proceedings: International Scientific Conference MITECH*, ČZU, Praha, 2008.